Egypt.J.Chem. **Vol. 62**, No. 3 pp. 487 - 500 (2019)

An Improved Sensitive and Selective Non-enzymatic Glucose Biosensor Based on PEG Assisted CuO Nanocomposites

A. Mohamed Azharudeen[1], T. Suriyakala[1], M. Rajarajan[2*], A. Suganthi[3]

[1]PG and Research Department of Chemistry, C.P.A. College, BBodinayakanur - 625513, Theni District, TamilNadu, India.

[2]Directorate of Distance Education, Madurai Kamaraj University, Madurai-625021. TamilNadu, India.

[3]Mother Teresa Women's University, Kodaikanal - 624 102, Dindugal District. TamilNadu, India.

DETERMINATION of glucose is of enormous importance in the fields of biological, environmental and clinical analyses. In recent years, polymer modified metal oxides arrived a great consideration in the detection of glucose. In this study, we have developed a sensitive and selective non-enzymatic glucose sensor by using CuO NMO encapsulation with PEG (poly ethyleneglycol) nanocomposites. The loading content of PEG was incorporated with CuO by weight percentage (wt = 2, 4 & 6%). The fabricated CuO/PEG nanocomposites were utilized as a glucose sensor, it exhibits the tremendous electrocatalytic performances on oxidation of glucose. The electrocatalytic activity enhances with increasing the loading of PEG content. The sensor shows a low detection limit of 0.25 µM with a sensitivity of 113.8 µA mM^{-1} cm^{-2}, good selectivity and stability. The CuO/PEG nanocomposites are hopeful for the advancement of cost-effective non-enzymatic glucose biosensors.

Keyword: CuO, Mesoporous, PEG, Glucose, Biosensor.

Introduction

The enlargement of electrochemical glucose sensor has fascinated extensive awareness in many areas such biotechnology, clinical diagnostics and food industry [1-3]. Blood glucose observation is a mode of testing the concentration of glucose in the blood and particularly essential in the protection of diabetes. In the past, the investigation for the enzymatic glucose biosensors based on using glucose oxidase have been extensively employed in the glucose determination was very popular owing to their high sensitivity, selectivity and low detection limit [4-6]. Clark et al., [7] discovered enzyme based first electrode system for monitoring in cardiovascular surgery and afterwards there are numerous enzyme oriented electrode was designed. However, enzyme oriented glucose biosensors undergo several disadvantages such as inadequate stability originated from the thermal and chemical instability of enzymes, intricate immobilization route of enzyme, poor reproducibility, high cost and the oxygen limitation [8,9].

To solve this trouble, numerous endeavours have been made to build up non-enzymatic glucose sensor. It is predominantly based on the glucose oxidation catalyzed by a multiplicity of electrocatalysts. The noble metals and metallic alloy are frequently utilized as catalytic materials for non-enzymatic glucose sensor. Among the noble metals, Cu and its oxides have gained an increasing awareness owing to their high electrocatalytic activity, low cost and anti-poisoning of chloridion, opportunity of promoting electron transfer reaction at a lower over potential [10,11]. For instance, Wang *et al.,* synthesised CuO nanomaterials for the application of non-enzymatic glucose sensor [12]. Though, there are several attempts for preparing homogeneous nanoparticles and nanostructured metal oxides (NMOs) applied in the field of glucose sensor, due to their high oxidation potential, low sensitivity and fouling of the oxidation signals [13], the researchers travel to nanocomposites material for resolve these problems.

*Corresponding author e-mail: rajarajanchem1962@gmail.com; Phone: 0452 - 2459413; Fax: 0452-2458261

DOI: 10.21608/EJCHEM.2018.5707.1489

In the production of nanocomposite materials, the polymer plays huge attention in electrochemical sensor because of unique properties of polymer such as compatibility, conductive nature, electron promoter and inexpensive [14,15]. The polymers such as poly (ethylene glycol) (PEG) [16], poly (vinyl pyrrolidone) (PVP) [17], poly vinyl alcohol (PVA) [18], poly acrylicacid (PAA) [19] and polyaniline (PANI) [20] are essentially used as binding mediator between the substrate and the glucose or a conductive substrate or as a adapted membrane for enhanced selectivity towards glucose [21]. It is well identified that, PEG has biocompatible lubricity and thermal stability. Hence, PEG was chosen as a capping or reducing agent in this work.

Besides, numerous researchers have been reported the preparation of nanocomposites using PEG as a surfactant/capping agent or modifier. Because, it is an economical organic stabilizer, simply soluble in water, need not difficult process, reactivity at relatively low temperature, non-toxic, non-irritating and moisturizing properties [22,23]. For instance, Reddy et al., [24] reported that, PEG modified MoO_3 nanobelts through hydrothermal synthesis, Wolcott et al., [25] explored the interaction of PEG with WO_3 and concluded the enhanced behaviour for PEG assisted nanoparticles in morphology, crystallanity and surface activity in addition to charge transport properties. Then, Wang et al., [26] reported that, one-step solid state reaction to the synthesis of copper oxide nanorods in the presence of a suitable surfactant (PEG), in this work the polymer PEG is used as a surfactant. Thus, previous reports obviously show that CuO based nanocomposites were rarely investigated to the development of glucose biosensor.

Here in, we report the preparation of CuO NMO via chemical precipitation method and incorporated with PEG. The fabricated CuO/PEG composites were applied as a highly reactive electrocatalyst for glucose oxidation. The sensor exhibits excellent performance such as high sensitivity, stability, low detection limit, good selectivity and cost effective.

Experimental

Reagents

$Cu(NO_3)_2$. $3H_2O$, NaOH, glucose, ethanol and PEG of analytical grade and purchased from Merck, India and were used without additional purification. All solutions were recently prepared with double distilled (DD) water.

Synthesis of copper oxide

About 2.4 g of copper nitrate trihydrate (0.1 M) is dissolved in 100 mL of DD water and 0.8 g of NaOH (0.2 M) is dissolved in 100 mL of DD water, separately. The copper nitrate trihydrate solution was taken in a RB flask and NaOH solution is added slowly drop by drop to the above solution under continuous magnetic stirring for 2 hrs. The precipitate is then filtered off and heated in a hot air oven at 120 ^oC for 1 hr. The product is finely crushed and calcinated at 500^oC for 2 hrs in a muffle furnace. The product obtained was black in colour.

Preparation of PEG modified CuO nanocomposites

The polymer modified copper oxide is prepared by immersion method. 2 g of earlier synthesized CuO in 100 mL of ethanol was immersed with 2% of PEG in ethanol using ultrasonication for 1 hr. After 12 hrs stirring the solvent is evaporated and product was dried at 80^oC followed by a heat treatment at 160^oC in a hot air oven for 2 hrs. Similarly, 4% of PEG and 6% of PEG in ethanol was immersed with CuO NMO successively.

Preparation of modified CuO/PEG/GCE biosensor

Preceding to use, the glassy carbon (GC) electrode was carefully polished with polishing paper and 1.0, 0.3 and 0.05 mm alumina slurry consecutively then dried in air after that sonicated in DD water followed by ethanol meticulously. The electrode was sonicated for 10 min to remove the adsorbed alumina particles on the surface of the GC electrode. Then the electrode was washed with ethanol and subsequently with DD water and the 6 mg of synthesized CuO/2%PEG was dispersed with DD water (3 mL) and ethanol (2 mL) using ultrasonically dispersion. Then approximately 5 µL of dispersion was dipped onto the clean GC electrode and dried at room temperature. The modified CuO/2%PEG(C2P)/GC electrode was attained. Similarly, the CuO/4%PEG(C4P)/GC modified electrode, CuO/6%PEG(C6P)/GC modified electrode, CuO/GC modified electrode and PEG/GC modified electrode were also obtained successively.

Characterization

The absorption of synthesized nanocomposites are determined by using JASCO V-750 spectrophotometer, the functional group was predicted by JASCO FT/IR-4200 Fourier-Transform spectrophotometer. The crystalline structure of synthesised nanomaterial was

confirmed by Analytical XPERT PRO X-ray diffractometer with Cu Kα radiation of wavelength 1.541. The SEM & EDX results of synthesized nanocomposites are analyzed by JOEL model JSM 6701FSEM. The HR-TEM & SEAD images attained from JOEL model 3010 microscope. The surface area is measured by micromatrics, ASAP 2020 B.E.T instrument.

Electrochemical experiments of synthesised nanomaterials CuO, C2P, C4P and C6P were performed with a CHI608D electrochemical workstation (CHI, USA). A standard three electrode cell was employed for the electrochemical tests. A 3-mm diameter GC was used as the working electrode (a working area of around 0.07 cm^2). A silver/silver chloride (Ag/AgCl) electrode and a platinum electrode were utilized as the reference and the counter electrodes, respectively. All potentials in this examine are accounted with respect to the Ag/AgCl electrode. The measurements were carried out in a 0.1 M NaOH solution on a pH of 12 at room temperature.

Results and Discussion

UV-vis-DRS

The optical property is very important in the field of electrocatalytic activity. The UV-vis-DRS of CuO, C2P, C4P and C6P nanocomposites are shown in Fig. 1. The absorption edge of CuO found at 360.08 nm, whereas, the polymer modified composites C2P, C4P and C6P were existed at 361.84, 362.01 and 364.75 nm respectively. The CuO NMO was compared with the C2P, C4P and C6P are slightly red shifted from 360.08 to 361.84, 362.01 and 364.75 nm respectively.

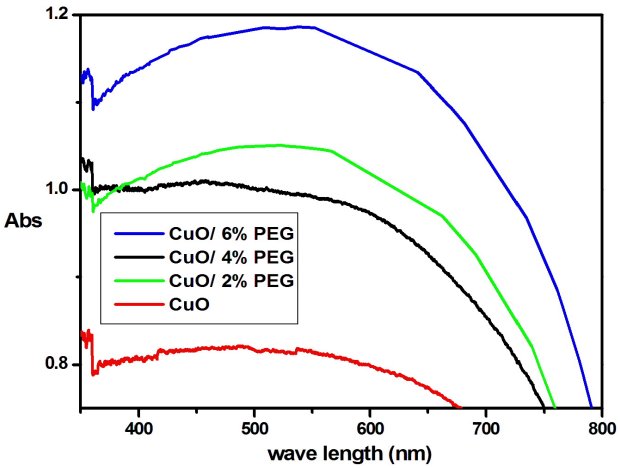

Fig. 1. UV- vis DR spectrum of CuO, C2P, C4P and C6P nanocomposites.

This observed red shift is revealed that the electron transfer process is taking place in composite materials. The polymer enhances the electron transfer from valance band to conduction band by overlapping or capping on surface of the CuO This red shift leads to the increase in grain size and electro active sites of synthesized nanocomposites of C2P, C4P and C6P, while increase in PEG content. Among, the synthesized composite C6P having high in shift. Therefore, high in granular size, more effective area and high electrocatalytic activity. The energy band gaps of CuO, C2P, C4P and C6P were determined by using Tauc's equation (1).

$$\alpha = \frac{C(h\nu - E_g\, bulk)^2}{h\nu} \qquad (1).$$

Where α, C, $h\nu$ and E_g^{bulk} are absorption coefficient, constant, photon energy and band gap, respectively. Tauc's plots of CuO, C2P, C4P and C6P are given in Fig. 2. The optical band gaps are 3.42, 3.34, 2.94 and 1.42 eV for CuO, C2P, C4P and C6P, respectively. It is found that, the loading of PEG was increased with decreasing the band gap energy ($E_{g)}$. This may be due to the increase of oxygen deficiency while increase the PEG concentration without changing the concentration of CuO. This specified that the PEG embraced samples have more optical conductivity than the surfactant free sample.

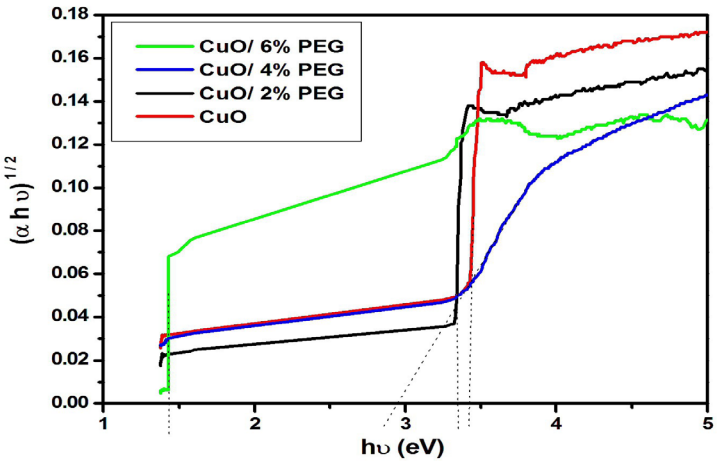

Fig. 2. Tauc's plot of C, C2P, C4P and C6P nanocomposites.

Fourier-Transform Infrared (FT-IR)

The FT-IR spectrum of prepared CuO, C2P, C4P and C6P nanocomposites are shown in Fig. 3 (a-d). The characteristic peak of 610.45, 614.61, 619.22 and 627.74 cm^{-1} in the spectrum of CuO, C2P, C4P and C6P shows the bending vibration of the CuO crystal lattice [27]. The spectrum of C2P, C4P and C6P nanocomposites were compared with CuO NMO, the wave numbers shifted from 610.45 to 627.74 cm^{-1}. This shift demonstrates that, the presence of CuO in the PEG matrix. Further, the peaks appeared at 445.60, 452.67, 508.10 and 526.01 cm^{-1} of CuO, C2P, C4P and C6P respectively, belongs to the Cu-O deformation vibration. The absorption band at 1388.20 cm^{-1} for the sample of C6P (Fig. 3d) spectra corresponds to the bending vibration of methylene ($-CH_2$) while the loading of PEG is high (6%), and this result suggested that some PEG molecules absorb on the surface on the CuO NMO, when increasing the loading of PEG. But, in case of C2P and C4P spectrum there is no absorption peak in the range of 1380 to 1395 cm^{-1}. Since, low level loading of polymer (PEG) leads to the poor interaction between CuO NMO.

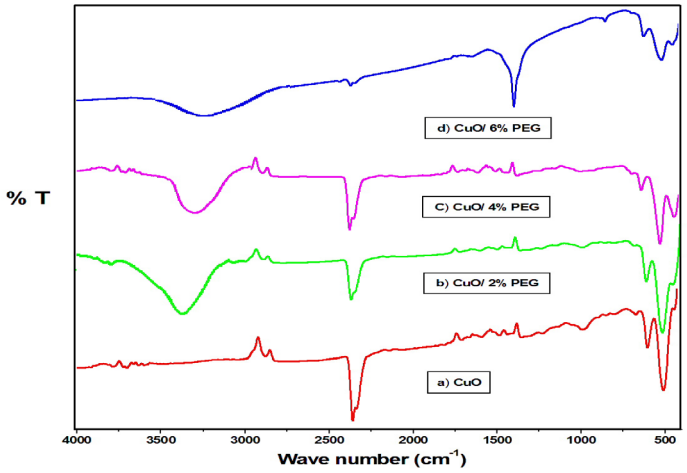

Fig. 3. FT-IR spectrum of (a) C, (b) C2P, (c) C4P and (d) C6P nanocomposites.

The broad peak at 3379.43, 3309.71 and 3253.90 cm^{-1} corresponds to the stretching mode of –OH group of CuO capped PEG named as C2P, C4P and C6P. Once again, this shift reveals that the formation of inter molecular hydrogen bonds by the –OH of PEG on the surface of CuO NMO [28], thereby confirming the capping of PEG on CuO NMO. Here, the wave number decreases while the concentration of PEG increases onto the CuO NMO. Hence, the PEG encapsulate on the surface of CuO NMO.

X-Ray Diffraction (XRD)

The X-ray diffraction patterns of CuO and after loading of PEG different content of C2P, C4P and C6P were shown in Fig. 4 (a-d). The XRD pattern of CuO (Fig. 4a) is compared with all polymer modified nanocomposites such as C2P, C4P and C6P can keep the typical CuO crystal structure after CuO NMO are incorporated into the PEG. In contrast with the standard diffraction patterns for C (JCPDS NO. 41-0254). Meanwhile no other diffraction peaks for impurities are detected. The diffraction peaks attain at 2θ values of 32.52°, 35.51°, 38.93°, 46.38°, 48.75°, 53.51°, 58.37°, 61.65°, 66.32°, 67.87°, 72.44° and 74.89°, corresponding to (110), (-111), (200), (-112), (-202), (020), (202), (-113), (-311), (113), (311) and (004), respectively, can be indexed to the monoclinic phase of CuO [29] with lattice constants a = 4.685 Å, b = 3.423 Å and c = 5.132 Å. The XRD patterns also illustrated that, the intercalation of PEG does not vary the crystal structure of monoclinic CuO NMO. When the loading content of PEG was increased with decreasing in the intensity of diffraction peaks. This renders that incorporation of PEG on the surface of CuO NMO. The sharp diffraction peaks indicate excellent crystal structure of prepared CuO NMO. The average crystallite size is determined by Scherrer's formula given in below (eq. 2)

$$D = \frac{K\lambda}{\beta \cos\theta} \qquad (2)$$

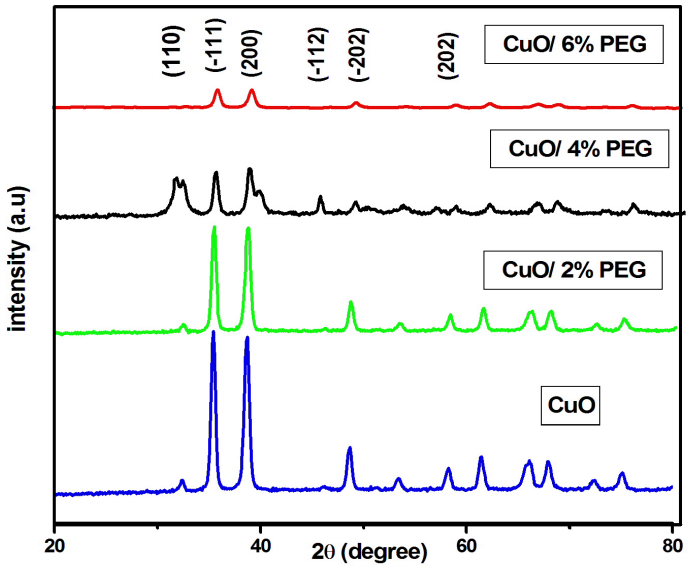

Fig. 4. XRD pattern of (a) C, (b) C2P, (c) C4P and (d) C6P nanocomposites.

Where *D* is the average crystallite size, *β* is the full width half maximum (FWHM) of the 2θ peak. *K* is the shape of factor of the particles (it equals to 0.89), *θ* and *λ* are the incident of angle and wavelength of the X-rays. The crystallite sizes were determined as 10.79, 12.08, 14.83 and 44.94 nm for CuO, C2P, C4P and C6P, respectively. This result reveals that, there is a change in crystallite size. Obviously, this shows the capping effect of PEG on CuO NMO.

Surface morphology and micro structure

The surface morphology of synthesized nanomaterials CuO, C2P, C4P and C6P are characterized by SEM and exhibited in Fig. 5 (a-d). The CuO NMO (Fig. 5a) possesses irregular rod as well as sphere like structure and the surface is rough. However, after loading of PEG the C2P nanocomposites (Fig. 5b) the surface morphology became needle like structure. The nanocomposites of C4P (Fig. 5c) resembled with nanorod and nanoflakes

with smooth surface and the C6P nanocomposites (Fig. 5d) revealed that, the nanorod and nanoflake like structure with bigger in diameter derived from CuO NMO, illustrating the polymerization of the poly ethylene glycol (PEG) takes place on the surface of the CuO NMO. This image is depicted in Fig. 5 (d). The HR-TEM images of C6P nanocomposites (Fig. 6 a-c) show petal like structure and good dispersion of the nanoparticles within the polymer matrix of PEG. Figure 6 (d) displayed the selected area diffraction pattern (SAED), it shows the crystallinity of C6P nanocomposites.

The existence of Cu and O was confirmed by EDX and the results are given in Fig. 7 (a-d). The EDX results confirm the presence of Cu and O. The peaks relevant to Cu and O are apparently observed at their normal energy. The EDX spectral data indicates obviously the formation of CuO NMO. It is found that, the intensity of the Cu in the EDX spectrum of CuO is 1464 increases to 1628, 2473 and 2743 for the EDX spectrum of C2P, C4P and C6P nanocomposites respectively, while the PEG content is increasing. This confirms the polymer PEG exists on the surface of the CuO NMO.

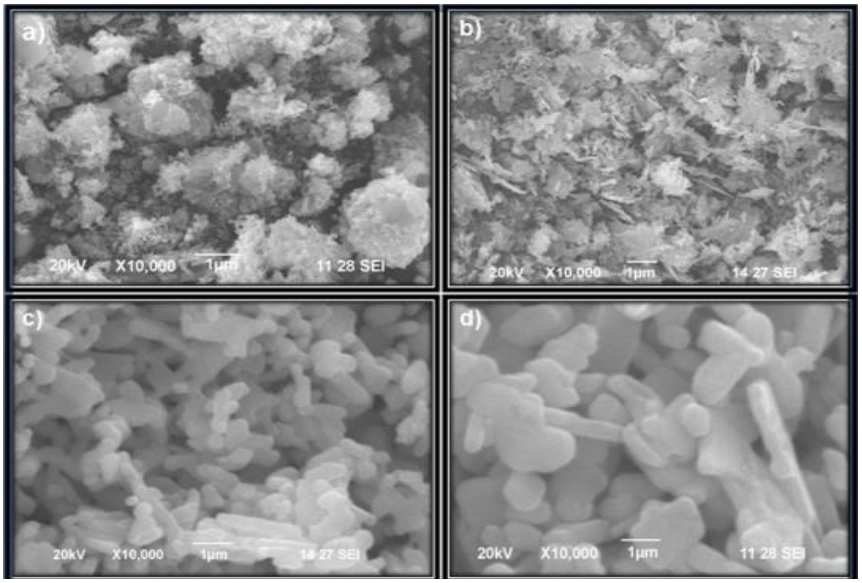

Fig. 5. SEM images of (a) C, (b) C2P, (c) C4P and (d) C6P nanocomposites.

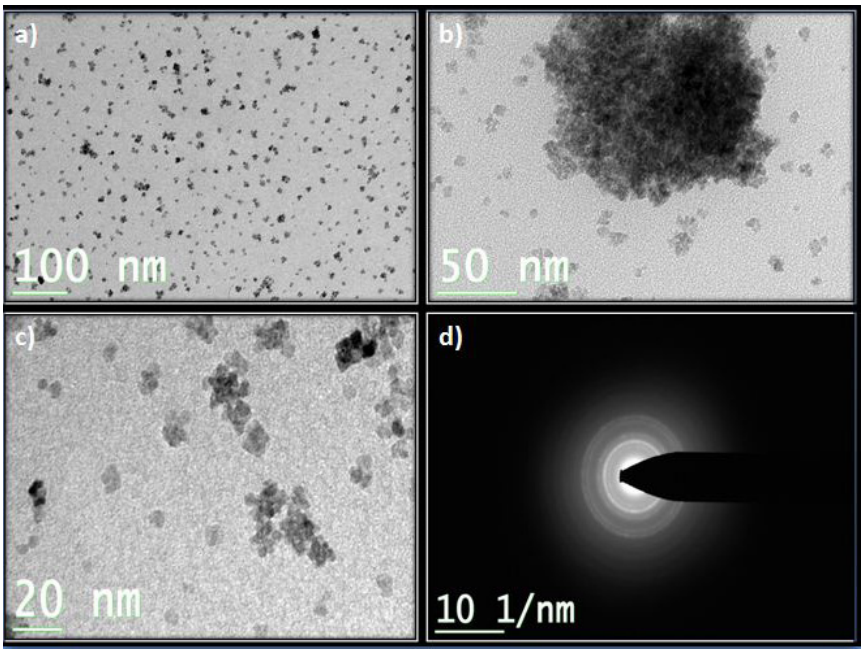

Fig. 6. HR-TEM (a-c) & SEAD (d) images of C6P nanocomposites.

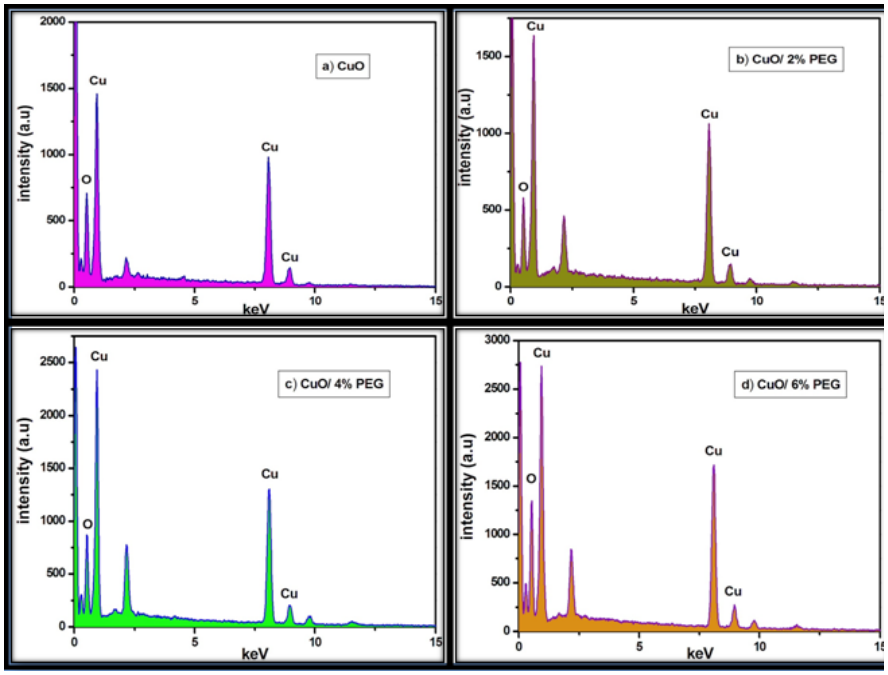

Fig. 7. The EDX spectrum of (a) C, (b) C2P, (c) C4P and (d) C6P nanocomposites.

Brunauer–Emmett–Teller (BET) adsorption-desorption isotherm

N_2 adsorption-desorption analysis is used to evaluate pore structures and surface area of CuO before and after loading of PEG based on the BET method. Figure 8 (a-d) is displayed the N_2 adsorption-desorption curves of CuO, C2P, C4P and C6P, respectively measured at 77 K. The surface areas were found to be 5.72, 16.39, 33.92 and 57.34 m^2/g for CuO, C2P, C4P and C6P respectively. The N_2 adsorption-desorption curves of CuO (Fig. 8a) is compared with, the C2P (Fig. 8b) and C4P (Fig. 8c) obeys the reversible type-III adsorption isotherm including CuO. Here, the interaction (adsorptive-adsorbent) between N_2 gas on CuO, C2P and C4P are weak. However, this type of isotherms is not common, because, the small pore of CuO, C2P and C4P does not fill with the adsorbate N_2 gas. These are typical features of non-porous and macroporus materials. However, the C6P (Fig. 8d), the adsorption isotherm obviously followed type-IV and exhibits distinct hyderesis loop and indicating mesoporous. This type of isotherm taking place in mesopores materials. The adsorbent C6P have large surface area having more active sites, it allows the adsorbate N_2 gas on its surface area in complete pore filling [30], while the loading of PEG is increased to 6%. The polymer PEG plays a major role, it acts as a mesoporous medium to allow a guest molecule on its surface.

Among, the prepared nanocomposite C6P having more surface area and active-sites supplied by the polymer PEG, it might have large sensing activity. The sensitivity of the nanocomposites attributed to the nature of polymer, which serve as a matrix to oxidize the glucose molecule.

Electrochemical performance of modified electrodes

The modified electrode was characterized by cyclic voltammetry (CV) between the potential of -0.4 to 0.7 V in 0.1M NaOH solution at 50 mV s^{-1} scan rate. The cyclic voltammogram of CuO shows in Fig. 9. The anodic peak current of CuO is appeared at 0.5 µA. This is owing to the electrocatalytic oxidation process in the alkaline electrolyte at the CuO electrode is generally considered as the following step:

The CuO is electrochemically oxidized to strong oxidizing Cu(III) species that is CuOOH is formed.

The other electrodes, such as PEG/GC electrode, C2P/GC electrode, C4P/GC electrode and C6P/GC electrode were conducted in 0.1M NaOH solution at 50 mV s^{-1} scan rate. As shown in Fig. 9(a) no redox peaks can be observed at the GC electrode and PEG modified GC electrode. However, increase in current can be observed at around 0.4 V (vs Ag/AgCl) on the anodic peak current of 1.05, 1.24 and 1.89 µA for C2P/ GC electrode,

C4P/GC electrode and C6P/GC electrode, respectively. Among these results, the C6P/GC electrode has higher capacitance than the others. This indicate that the CuO have greatly improved the performance of the electrode and increased the electrocatalytic ability by increasing the loading content of PEG towards glucose oxidation, which may also be ascribed to their large surface area, active sites and enhanced the electron transfer rather than other electrodes.

Effect of glucose concentration

Furthermore, we used the same C6P/GCE to detect glucose molecule with various concentrations between 2 to 12 mM glucose in 0.1 M NaOH medium at the scan rate of 25 mV s^{-1}. As shown in Fig. 9 (b), the oxidation current can be found between 0.30 and 0.6 V. The anodic peak is altered to the high potential region while the glucose concentration is increased. For the detection of 12 mM glucose, the peak current of a C6P modified GC electrode can reach 2.55 µA. However, the peak current for 14 mM glucose is lower than 12 mM glucose. Because, there is a degradation or fatigue occurrence for repetitive measurements using the same one electrode. The electrocatalytic oxidation process of glucose molecule by modified GCE in alkaline electrolyte undergoing several steps:

The glucose is catalytically oxidized by the Cu(III) species and produces gluconic acid.

Effect of Scan rate

The influence of scan rate on glucose oxidation at the C6P/GC modified electrode was also investigated in 0.1 mM glucose for the understanding of the oxidation process. Figure 9(c) reveals that the CV of C6P/GC electrode in the range of 5-50 mV s^{-1}. The oxidation peak current increased progressively with increasing the scan rate. As shown in the inset of Fig. 9 (c) linear response with the peak current (I_{pa}) and the scan rate (ν) with a correlation coefficient(R^2) of 0.9964. The linear regression equation is expressed as I_{pa} (µA) = 2.33 + 4.06 ν (mV s^{-1}). This result verifies that the electrochemical oxidation of glucose is controlled by surface adsorption of glucose molecule.

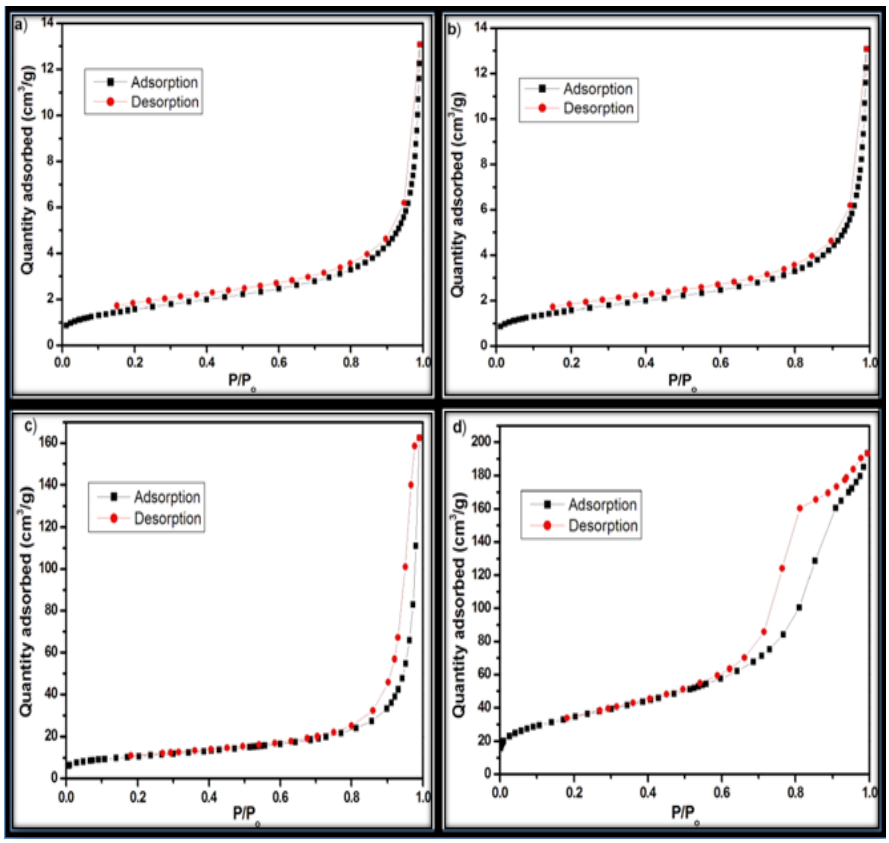

Fig. 8. N2 adsorption-desorption isotherm for (a) C, (b) C2P, (c) C4P and (d) C6P nanocomposites

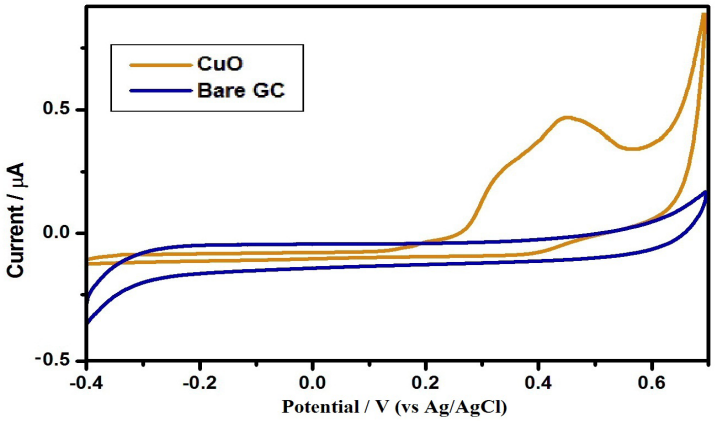

Fig. 9. CV curve of CuO modified GCE in 0.1 M of NaOH solution at the scan rate of 50 mVs-1.

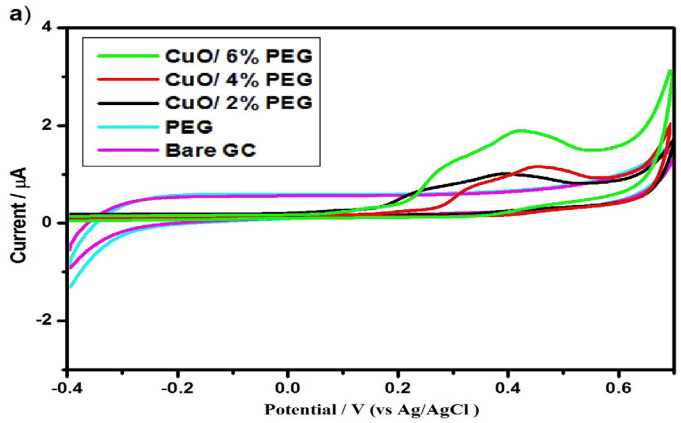

Fig. 9 (a). CV curves of PEG, C2P, C4P and C6P modified GCEs in 0.1 M of NaOH solution at the scan rate of 50 mVs-1.

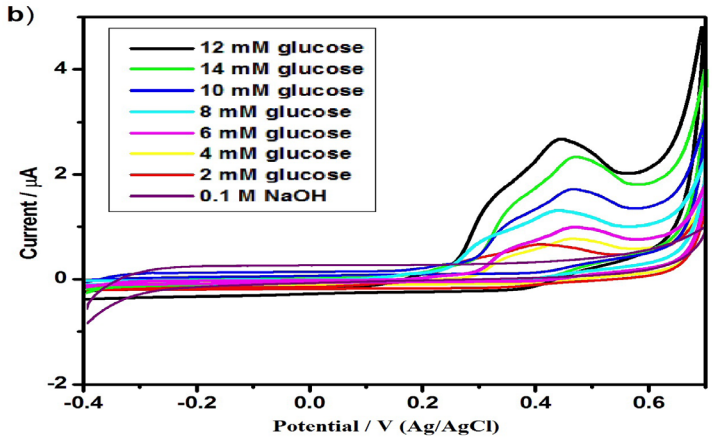

Fig. 9 (b). CV curves of C6P modified GCE under various glucose concentration in 0.1 M of NaOH solution at the scan rate of 25 mVs-1.

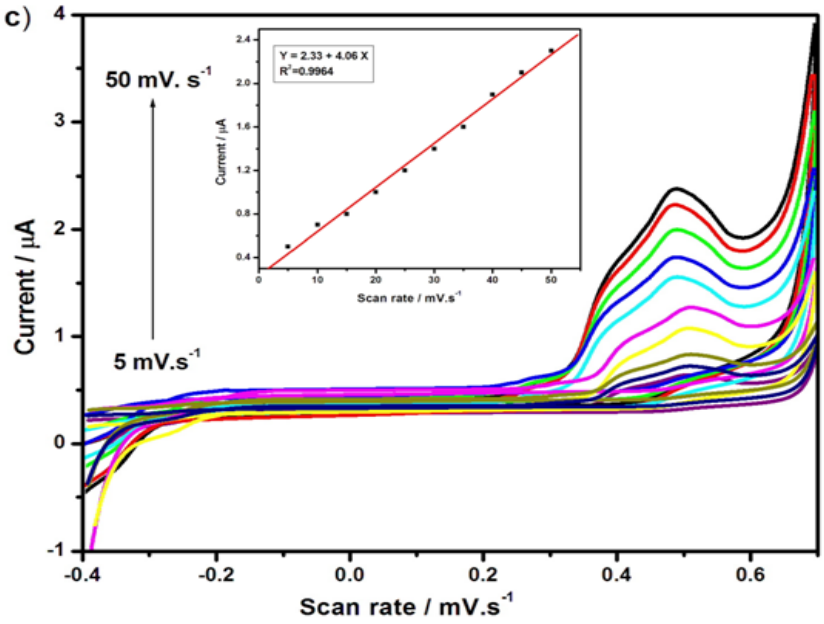

Fig. 9 (c). Give to supporting CV of 5 mM glucose at the different scan rate. Inset: The plot of anodic peak currents vs. Scan rates.

Amperometric detection of glucose at C6P/GCE

Amperometry was utilized to ascertain the detection of glucose. The 0.1 M NaOH was used as the supporting solution with the injection of 2 µM glucose every 25 s. The potential was set as +0.4 V (vs. Ag/AgCl) since, in Fig. 9 (b) the current response of C6P increased gradually from +0.4 to +0.6 V. From Fig. 9 (b) the anodic peak current exists between +0.4 V to +0.6 V. The optimum applied potential may be present in the range of +0.4 to + 0.6 V. But, the potential of +0.4 was 1 fold larger than +0.3 V and 2 fold smaller than +0.6 V. Therefore, the applied potential was fixed as +0.40 V and the result shown in Fig. 10. From the amperometric curve of glucose, the current increases gradually. The linear relationship between the oxidation current and the glucose concentration was obtained for concentrations ranging from 2 µM to 18 µM. Figure 11 showed that, the amperometric response of each addition of 20, 40, 60, 80 and 100 µM. The insets of Fig. 10 and 12 show the corresponding calibration curve of the sensor. The linear equations I_{pa} (A) = 5.00 + 2.73 $C_{glucose}$ and I_{pa} (A) = 3.59 – 4.41 $C_{glucose}$ with correlation coefficient (R^2) of 0.9912 and 0.9976 was obtained, respectively. Under the optimal conditions the sensor shows a low detection limit (S/N=3) of 0.25 µM with a sensitivity of 113.8 µA mM^{-1} cm^{-2}. This high level of the sensitivity is mainly attributed to the electrocatalytic activity of CuO with the enhancement effect of polymer PEG, which acts as a network to oxidize the glucose molecule.

Interference Analysis

It is well known that some simply oxidative species such as fructose, sucrose, uric acid (UA) and ascorbic acid (AA) frequently co-exist with glucose in human blood [32]. Thus, the electrochemical reply of the interfering species also examined at the C6P/GCE, as shown in Fig. 13. As shown in Fig. 13, no significant signals can be observed for interfering species such as 0.1 µM of fructose, 0.1 µM of sucrose, 0.1 µM ureic acid (UA) and 0.1 µM of ascorbic acid (AA)., while the addition of 1 µM of glucose the oxidation peak current on C6P/GCE increases from 3.52 to 4.44 µA. This indicates that C6P/GCE exhibit good selectivity towards glucose sensing. Hence, it is clear that the composite electrode has low sensitivity for the interfering species such as fructose, sucrose, uric acid and ascorbic acid.

The C6P modified GC electrode was exhibit a relatively wide linear range, low detection limit, high sensitivity, good selectivity and stability. The proposed polymer assisted C6P nanocomposite based non-enzymatic glucose sensor may have potential for the analysis of glucose in real samples. A performance comparison of our sensor with other nonenzymatic glucose sensors is summarized in Table 1.

The repeatability and storage stability of glucose sensor were also evaluated at the same modified electrode over consecutive 30 days. When the modified electrode is not used, it is stored in air. After two weeks, the current reply of C6P modified electrode just losses 1.1% of its original current. The good reproducibility and long term stability of CuO/PEG/GC electrode are owing to the chemically stable CuO phase intercalated with PEG network. Thus, the observed actions of the proposed glucose sensor using CuO/PEG nanocomposite showed a good selective response for the detection of glucose.

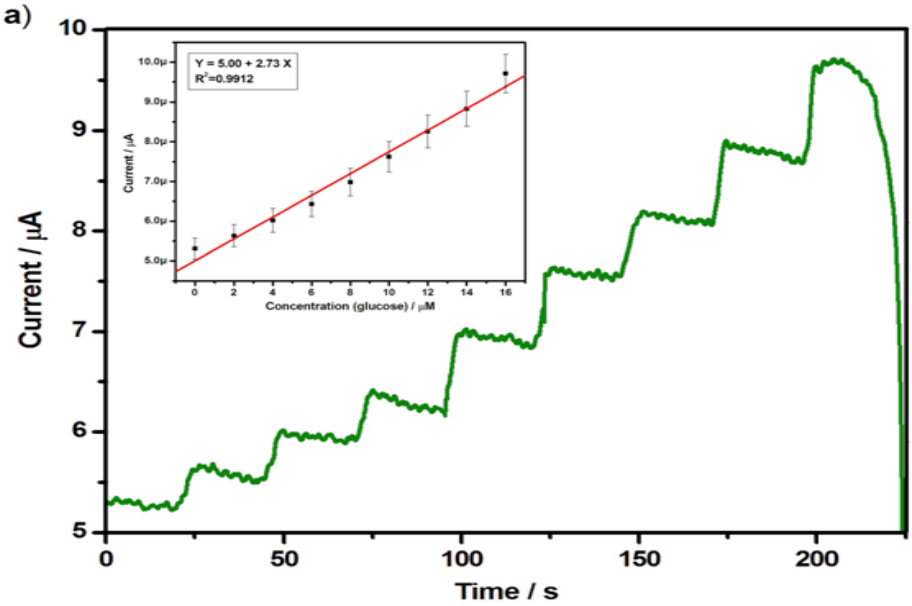

Fig. 10. Amperometric response of C6P modified GCE biosensor with the successive addition of each 2 µM glucose in 0.1 M of NaOH measured at +0.40 V. Insets: Corresponding calibration curve between the current and concentration of glucose.

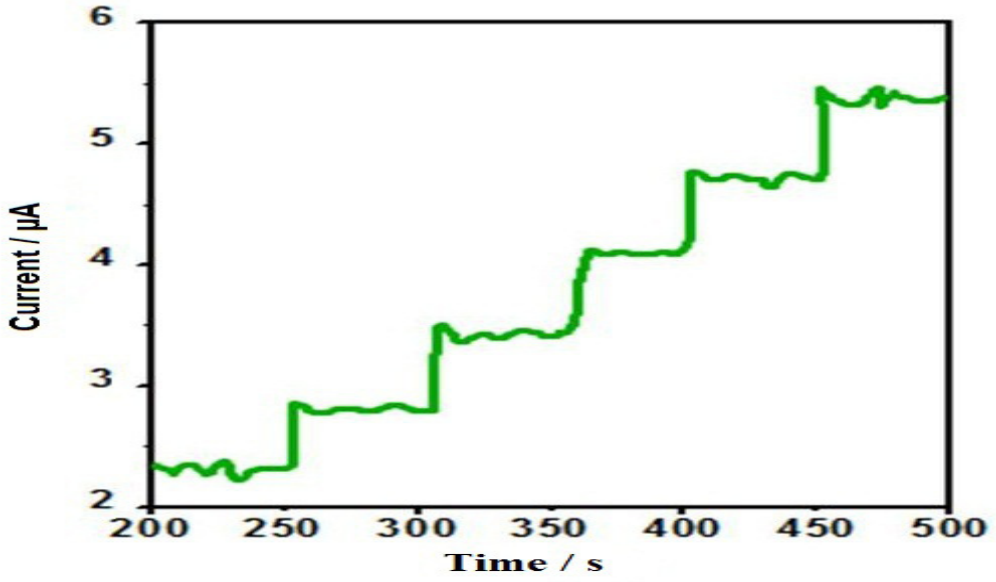

Fig. 11. Amperometric response of C6P modified GCE biosensor with the range of 20 to 100 µM glucose in 0.1 M of NaOH, Eapp = + 0.40 V.

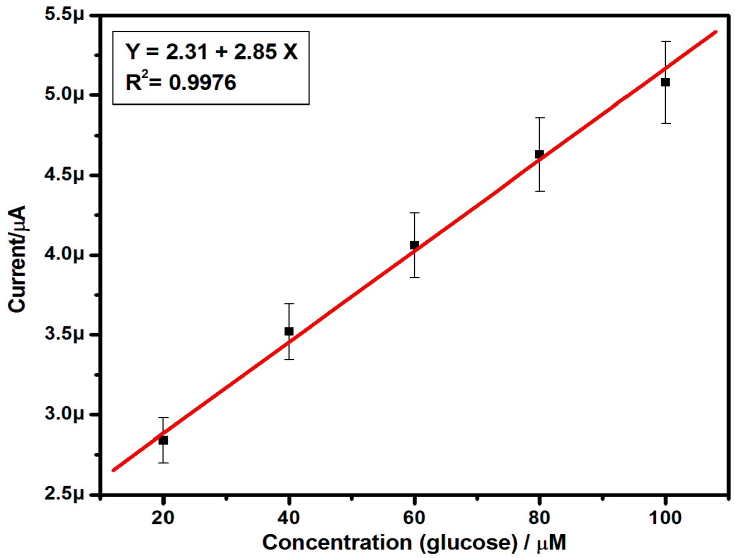

Fig. 12. Calibration curve between the current and concentration of glucose for amperometric response in the range of 20 to 100 µM .

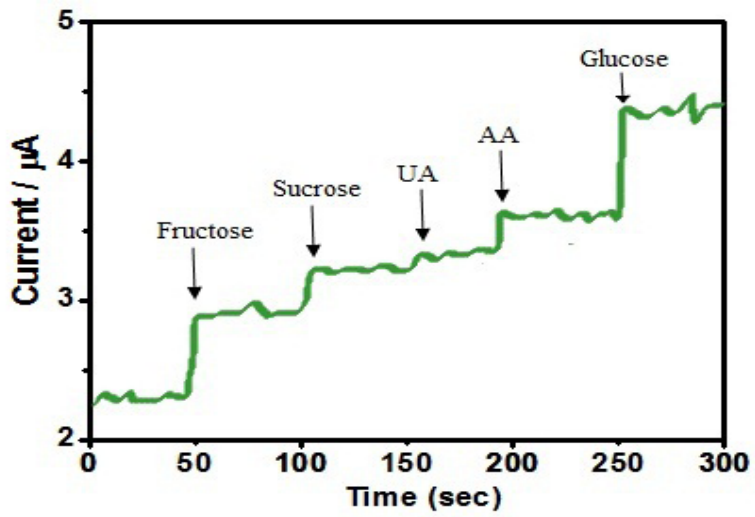

Fig. 13. Interference analysis of the sensor in 0.1 M NaOH at +0.40 V with 1 µM glucose and other interferents including 0.1 µM of fructose, 0.1 µM of sucrose, 0.1 µM ureic acid (UA) and 0.1 µM of ascorbic acid (AA).

TABLE 1. Comparison of some bio sensing activity of other modified electrodes with CuO/PEG/GCE.

S. No	Working electrode	Detection limit	Linear range	References
1	Pd- SMNT	0.2 ± 0.05 µM	0.5 - 17 mM	[32]
2	CuO nanowires	4.9 µM	0.0004 - 200 mM	[33]
3	Porous Au	5 µM	2 -10 mM	[34]
4	Cu/MWCNT	0.00021 mM	0.0007 - 3.5 mM	[35]
5	Ni-Cu/TiO_2 nanotubes	5 µM	3.2 mM - 10 µM	[36]
6	CuO/PEG/GCE	0.25 µM	up to 100 µM	This work

Conclusion

We have successfully synthesized copper oxide NMO through co-precipitation method. The synthesized CuO NMO was modified by using PEG as a capping or surfactant. The UV-vis-DRS show the optical conductivity of synthesized nanocomposites. The powder XRD investigation confirmed that the sample prepared with and without PEG in monoclinic structure corresponding to CuO. The SEM image of C6P shows that the formation of nanorods. The HR-TEM and SAED images show that, the petals like structure and good dispersion of crystallite CuO NMO within the polymer matrix. The EDX spectrum confirms the presence of Cu and O. The BET results exhibit that the modified NMO possess high surface area due to mesoporus. The C6P/GCE exhibited high electrocatalytic activity in the direction of the oxidation of glucose. The proposed method for glucose determination revealed that higher sensitivity and lower detection limit of 0.25 μM (S/N=3) with a sensitivity of 113.8 μA mM^{-1} cm^{-2}. The main reasons are the large surface area and good electrocatalytic activity of C6P nanocomposites, the polymer PEG enhanced the efficiency of the electron transfer between the modified electrode and glucose. The CuO/PEG/GCE also showed high stability, excellent selectivity and cost effective.

References

1. Wang J., Carbon- nanotubes based electrochemical biosensor: A review. *Electroanalysis*, **17**, 7-47 (2005).
2. Rivas G.A., Rubianes M.D., Rodriguez M.D., Ferreyra N.F., Luque G.L., Pedano M.L., Miscoria S.A., Carbon nanotubes paste electrodes. A new alternative for the development of electrochemical sensor, *Electroanalysis* **19**, 823-831 (2007).
3. Wang J., Electrochemical glucose biosensor, *Chem. Rev*. **108**, 814-825 (2008).
4. Qiu C.C., Wang X., Liu, Hou S.F., Ma H.Y., Direct electrochemistry of glucose oxidase immobilized on nanostructured gold thin films and its application to bioelectrochemical glucose sensor, *Electrochim. Acta* 67, 140-146 (2012).
5. Zeng J., Wei W., Liu X., Wang Y., Luo G., A simple method to fabricate a prussian blue nanoparticles/ carbon nanotubes/ poly (1,2- diaminobenzene) based glucose biosensor, *Microchim. Acta* **160**, 261- 267 (2008).
6. Umar A., Rahman M.M., Hajry A.A., Hahn Y.B., Enzymatic glucose biosensor based on flower-shaped copper oxide nanostructures composed of thin nanosheets, *Electrochem. Commun*. **11**, 278-281 (2009).
7. Clark L.C., and Lyons C., Electrode system for continuous monitoring in cardiovascular surgery, *Ann. N.Y. Acad. Sci*. **102**, 29-45 (1962).
8. Park S., Boo H., Chung T.D., Electrochemical non-enzymatic glucose sensors, *Anal. Chim. Acta* **556**, 46-57 (2006).
9. Tsai T.W., Heckert G., Neves L.F., Tan Y.Q., Kao D.Y., Harrison R.G., Resasco D.E., Schimidtke D.W., Adsorption of gluxose oxidase onto single-walled carbon nanotubes and its application in layer-by-layer biosensors, *Anal. Chem*. **81**, 7917-7925 (2009).
10. Kalita G., Matsushima M., Uchida H., Wakita K., Umeno M., Graphene constructed carbon thin films as transparent electrodes for solar cell applications, *J. Mater. Chem*. **20**, 9713-9717 (2010).
11. Reitz E., Jia W.Z., Gentile M., Wang Y., Lei Y., CuO nanospheres based nonenzymatic glucose sensor, *Electroanalysis* **20**, 2482-2486 (2008).
12. Wang X., Hu C., Liu H., Du G., He X., Xi Y., Synthesis of CuO nanostructures and their application for nonenzymatic glucose sensing, *Sens. Actuator B: Chem*. **144**, 220-225 (2010).
13. Chen A., and Chatterjee S., Nanomaterials based electrochemical sensor for biomedical applications, *Chem. Soc. Rev*. **42**, 5425-5438 (2013).
14. Bobacka J., Ivaska A., Lewenstam A., Potentiometric ion sensors based on conducting polymers, *Electroanalysis* **15**, 366-374 (2003).
15. Adhikari B., and Majumdar S., Polymers in sensor applications, *Prog. Polym. Sci*. **29**, 699–766 (2004).
16. Kohler N., Sun C., Fichtenholtz A., Gunn J., Fang C., Zhang M.Q., Methotrexate-immobilized poly(ethylene glycol) magnetic nanoparticles for MR imaging and drug delivery, *Small* **2**, 785–792 (2006).
17. Lee H.Y., Lee S.H., Xu C., Xie J., Lee J.H., Wu B., Koh A.L., Wang X., Sinclair R., Wang S.X., Nishimura D.G., Biswal S., Sun S., Cho S.H., Chen X., Synthesis and characterization of PVP-coated large core iron oxide nanoparticles

as an MRI contrast agent, *Nanotechnology* **19**, 165101/1–165101/6 (2008).

18. Hariharan R., Senthilkumar S., Suganthi A., Rajarajan M., Photodynamic action of curcumin derived polymer modified ZnO nanocomposites, *Mater. Res. Bull.* **94**, 454-459 (2005).

19. Mo X., Wang C.Y., You M., Zhu Y.R., Chen Z.Y., Hu Y., A novel ultraviolet- irradiation route to CdS nano crystallites with different morphologies, *Mater. Res. Bull.* **36**, 2277-2282 (2001).

20. Chen M., Xie Y., Chen H., Qiao Z., Zhu Y., Qian Y., Templated synthesis of CdS/PAN composites nanowires under ambient conditions, *J. Colloid Interf. Sci.* **229**, 217-221 (2000).

21. Tian K., Prestgard M., Tiwari A., A review of recent advances in nonenzymatic glucose sensors, *Mater. Sci. Eng. C* **41**, 100-118 (2014).

22. Deepa M., Kar M., Singh D.P., Srivastava A.K., Ahamed S., Influence of polyethylene glycol template on micro structure and electrochromic properties of tungsten oxide, *Sol. Energy Mater. Sol. Cells* **92**, 170-178 (2008).

23. Sudha R., Senthilkumar S., Hariharan R., Suganthi A., Rajarajan M., Synthesis, characterization and study of photocatalytic activity of surface modified ZnO nanoparticles by PEG capping, *J. Sol-gel Sci. Technol*. **65**, 301-310 (2013).

24. Reddy C.V.S., Jr E.H.W., Wen C., Mho S.I., Hydrothermal synthesis of MoO_3 nanobelts utilizing poly(ethylene glycol), *J. Power Sources* **183**, 330-333 (2008).

25. Wolcott A., Kuykendall T.R., Chen W., Chen S., Zhang J.Z., Synthesis and characterization of ultrathin WO_3 nanodisks utilizing long-chain poly(ethylene glycol), *J. Phys. Chem. B* **110**, 25288–25296 (2006).

26. Wang W., Zhan Y., Wang G., One-step solid state reaction to the synthesis of copper oxide nanorods in the presence of a suitable surfactant, *Chem. Commun*. **8**, 727-728 (2001).

27. Ghanbari K., Babaei Z., Fabrication and characterization of non-enzymatic glucose sensor based on ternary NiO/CuO/Polyaniline nanocomposites, *Anal. Biochem*. **498**, 37-46 (2016).

28. Hariharan R., Senthilkumar S., Suganthi A., Rajarajan M., Synthesis and characterization of doxorubicin modified ZnO/PEG nanomaterials and its photodynamic action, *J. Photochem. Photobiol. B* **116**, 56-65 (2012).

29. Wang X., Liu E., Zhang X., Non-enzymatic glucose biosensor based on copper oxide-reduced graphene oxide nanocomposites synthesized from water-isopropanol solution, *Electrochim. Acta,* **130**, 253-260 (2014).

30. Zhao D., Wan Y., Zhou W., Ordered Mesoporous Materials, *Wiley Publication* 55-116 (2013).

31. Ensafi A.A, Abarghoui M.M., Rezaei B., A new non-enzymatic glucose sensor based on copper/ porous silicon nanocomposite, *Electrochim. Acta,* **123**, 219-226 (2014).

32. Meng L., Jin J., Yang G.X., Lu T.H., Zhang H., Cai C.X., Nonenzymatic electrochemical detection of glucose based on palladium- single walled carbon nanotube hybrid nanostructures, *Anal. Chem*. **81**, 7271- 7280 (2009).

33. Zhuang Z.J., Su X.D., Yuan H.Y., Sun Q., Xiao D., Choi M.M., An improved sensitive nonenzymatic glucose sensor based on a CuO nanowire modified Cu electrode, *Analyst* **133**, 126-132 (2008).

34. Li Y., Song Y.Y., Yang C., Xia X.H., Hydrogen bubble dynamic template synthesis of porous gold for nonenzymatic electrochemical detection of glucose, *Electrochem. Commun.* **9**, 981-988 (2007).

35. Kang X.H., Mai Z.B., Zou X.Y., A sensitive nonenzymatic glucose sensor in alkaline media with a copper nanocluster/multiwall carbon nanotube-modified glassy carbon electrode. *Anal. Biochem*. **363**, 143-150 (2007).

36. Li X., Yao J., Liu F., He H., Zhou M., Mao N., Xiaoa P., Zhang Y., Nickel/Copper nanoparticles modified TiO_2 nanotubes for non-enzymatic glucose biosensors, *Sens. Actuators B* **181**, 501-508 (2013).

(*Received* 16/10/2018;
accepted 20/11/2018)